What Factors Affect the D-5(0) Energy of Eu3+? An Investigation of Nephelauxetic Effects

ARTICLE *in* THE JOURNAL OF PHYSICAL CHEMISTRY A · MARCH 2013

Impact Factor: 2.69 · DOI: 10.1021/jp400247r · Source: PubMed

3 AUTHORS:

Peter Anthony Tanner
The Hong Kong Institute of Education
355 PUBLICATIONS **4,364** CITATIONS
SEE PROFILE

Yau-yuen Yeung
The Hong Kong Institute of Education
85 PUBLICATIONS **1,080** CITATIONS
SEE PROFILE

Lixin Ning
Anhui Normal University
63 PUBLICATIONS **425** CITATIONS
SEE PROFILE

THE JOURNAL OF PHYSICAL CHEMISTRY A

Article

pubs.acs.org/JPCA

What Factors Affect the $^5D_0$ Energy of Eu^{3+}? An Investigation of Nephelauxetic Effects

Peter A. Tanner,*[,†] Yau Yuen Yeung,[†] and Lixin Ning[‡]

[†]Department of Science and Environmental Studies, The Hong Kong Institute of Education, 10 Lo Ping Road, Tai Po, New Territories, Hong Kong S.A.R., P. R. China

[‡]Department of Physics, Anhui Normal University, Wuhu, Anhui 241000, P. R. China

Supporting Information

ABSTRACT: Relationships involving the interelectronic repulsion parameters, F^k (k = 2, 4, 6), the spin–orbit coupling constant, ζ_f, and J-mixing, with the $^5D_0$–$^7F_0$ energy, E, have been investigated for Eu^{3+} using various approaches. First, the linear relationship between E and the $^7F_1$ splitting (or the second rank crystal field parameter) is shown to be applicable not only to glasses but also to solid-state crystalline systems with Eu^{3+} site symmetry of C_2, C_{2v}, or lower. In these cases, the change in $^5D_0$–$^7F_0$ energy is mainly due to the J-mixing effect of ^7F_J (J = 2, 4, 6: most notably J = 2) which depresses $^7F_0$, whereas the $^5D_0$ energy is relatively constant. The $^5D_0$–$^7F_0$ energy also depends upon certain energy parameters in the Hamiltonian, in particular, F^k and ζ_f. Model calculations show that increase in F^4 or F^6 produces an increase in E, whereas increase in F^2 produces a decrease in E. An increase in ζ_f produces a decrease in E. These findings are rationalized. Most previous $4f^6$ crystal field calculations have only considered the F and D terms of Eu^{3+} so that the Slater parameters are not well-determined. More reliable energy level data sets and crystal field calculations for Eu^{3+} with fluoride, oxide, or chloride ligands have been selected, and certain of these have been repeated since most previous calculations have errors in matrix elements. The fitted Slater parameters have been corrected for the effects of three-body Coulomb interactions. Some systems do not follow the ligand trend F ~ O > Cl for Slater and spin–orbit parameters. From the limited data available, the average values of the corrected Slater parameters are greater for fluoride compared with chloride ligands, but the differences are comparable with the standard deviations of the parameters. There is no clear nephelauxetic series for these three types of ligands, with respect to spin–orbit coupling. Previous correlations of E with various parameters are of limited value because the $^5D_0$–$^7F_0$ energy difference not only depends upon the F^k and ζ_f parameters but in addition is sensitive to the importance of J-mixing for low symmetry systems.

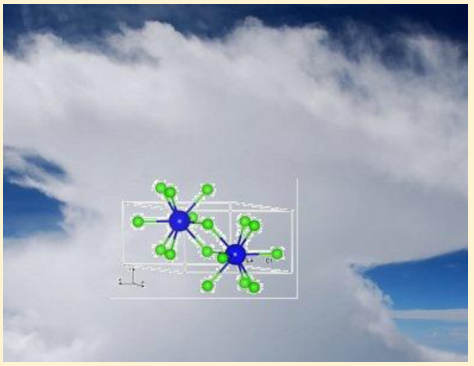

INTRODUCTION

The 3003 states of the $4f^6$ configuration of Eu^{3+} extend up to ~175000 cm^{-1}. The wave functions of the relevant states are described in an intermediate coupling basis as combinations of $^{2S+1}L_J$ multiplets. There are three ^5D_J multiplets for Eu^{3+}, with $^5D_0$ located at ca. 17200 cm^{-1} ($^5D(3)_0$) (hereafter, $^5D_0$), 42000 cm^{-1} ($^5D(2)_0$), and 75000 cm^{-1} ($^5D(1)_0$) (refer to the Supporting Information for details). The calculation of energy levels for the $4f^N$ configuration is most accurately performed by a semiempirical Hamiltonian comprising atomic (H_{AT}) and crystal field (H_{CF}) components:[1]

$$H = H_{AT} + H_{CF} \quad (1)$$

$$H_{AT} = E_{AVE} + \sum_k F^k \mathbf{f}_k + \sum_i \zeta_f \mathbf{s}_i \cdot \mathbf{l}_i + H_{ADD} \quad (2)$$

where k = 2, 4, 6; and i represents the sum over all 4f electrons. The first term in eq 2, E_{AVE}, adjusts the configuration barycenter energy with respect to other configurations. The Slater parameters F^k represent the electron–electron repulsion interactions and are two-electron radial integrals, where the $\mathbf{f}_k$ represent the angular operator part of the interaction. The spin–orbit interaction is represented by the next term in eq 2, and the constant ζ_f increases in magnitude across the lanthanide ion series. The Slater and spin–orbit coupling parameters are the most important in determining the atomic energies, and the additional terms, H_{ADD}, are subsequently discussed.

The nephelauxetic effect, literally "cloud-expanding" effect, concerns the red-shift of spectral features in complexes, relative to free ions. The shift has been associated with the decrease in interelectronic repulsion, quantified by the Racah parameter, B, for transition metal ions, and Jørgensen has provided the empirical relation for the ratio of interelectronic repulsion in a complex to that in the free ion.[2] Newman associated nephelauxetic shifts with changes in ligand polarizability and gave a linear relation of this quantity with the Racah parameter.[3] The shifts of spectral features of lanthanide ions

Received: January 9, 2013
Revised: March 7, 2013
Published: March 7, 2013

   dx.doi.org/10.1021/jp400247r | J. Phys. Chem. A 2013, 117, 2771–2781

have also been associated with nephelauxetic effects, namely, a reduction in magnitude of the Slater and spin−orbit coupling parameters with respect to the free ion values. The nephelauxetic series shows the magnitude of these shifts:[4]

$$\text{free ion} < F^- < O^{2-} < Cl^- < Br^- < I^- \sim S^{2-} \quad (3)$$

Jørgensen's concept was that the nephelauxetic effect arises from the reduction of 4f electron repulsion due to interpenetration of the ligand electron charge distribution.[4] Two models have been described, for example by Shen and Holzapfel,[5] to account for the 4f orbital "cloud expansion" in solids. The central field covalency model envisages that ligand electrons penetrate the 4f orbitals in a spherically symmetric manner to reduce f-electron interelectronic repulsion. By contrast, the symmetry-restricted covalency model treats the mixing of ligand and 4f electrons as a symmetry-dependent admixture. From a high-pressure study, these authors[5] found that linear relations exist between the average Eu−ligand distance and ζ_f or F^2, so that the central field covalency model was envisaged to be more appropriate for Eu^{3+}. Newman has argued that the reduction of Slater parameters is not due to covalency, since otherwise the crystal field parameters calculated using Hartree−Fock 4f orbitals would greatly underestimate the experimental values.[6] He suggested that the previous alternative mechanism involving the dielectric screening of the interelectronic repulsion by the crystal medium could account for the reduction of Slater parameters.[6]

In particular, various empirical relations have been provided to quantify the energy of the $^7F_0$−$^5D_0$ transition (with this *energy difference* frequently labeled E hereafter, for brevity) of Eu^{3+} in complexes compared with that of the free ion, in the context of the nephelauxetic effect. Albin and Horrocks[7] argued that since both of these levels are nondegenerate, the changes are due not to crystal field effects but indeed to the nephelauxetic effect. The equation,

$$E = -0.76p^2 + 2.29p + 17273 \quad (4)$$

was put forward from the study of the emission spectra of 36 complexes, with values of E differing by only 49 cm^{-1} (between 17226 and 17275 cm^{-1}), of which 11 were in the solid state and the remainder in solution. The stoichiometry of the complexes was not well-characterized. The parameter p represents the total charge on the ligands, and increasing negative charge produced lower E values. Amberger et al.[8] subsequently cited values of E in a much wider range, such as for $Ba_3Gd_2WO_3$:Eu^{3+} (17075 cm^{-1}); Y_6WO_{12}:Eu^{3+} (17370 cm^{-1}); $NaGdSb_2O_7$:Eu^{3+} at two sites (17333 and 17458 cm^{-1}); $Ca_{9.5}Eu_{0.5}(PO_4)_6O_{1.25}\square_{0.75}$ at two sites (17440 and 17510 cm^{-1}), and $Mg_3F_3BO_3$:Eu^{3+} (17615 cm^{-1}). These authors noted that when inserting E values from such systems into eq 4, the charges are represented by complex numbers.

Frey and Horrocks[9] used 27 determined $^5D_0$−$^7F_0$ energies, within the range of 55 cm^{-1}, mostly from aqueous solution, and without crystal structure data, to correlate E with the derived nephelauxetic parameters (δ_i) from the sum of n_i ligating atoms in Eu complexes:

$$E - 17374 = C \times \sum_i n_i\delta_i \quad (5)$$

and gave values of δ_i for 9 atom types, with 5 different coordination numbers (i.e., 45 data from 27 observables). The constant C was assigned a value for each coordination number from 7 to 11. This equation has been used many times in the literature in calculating E values for complexes and in many cases serious disagreement occurred. In those cases additional δ_i values were assigned to the atom type, depending upon its chemical environment.[10−13] Choppin and Wang[14] proposed the following correlation concerning the total ligand donor number, CN_L:

$$CN_L = 0.237(17276 - E) + 0.628 \quad (6)$$

based upon data from 20 organic ligand complexes in water or dimethyl sulfoxide. The spread of E values was 40 cm^{-1}, and structural data were not given concerning the coordination environment of Eu^{3+}. The low energy shift upon complex coordination was attributed to the nephelauxetic shift, arising from (i) increase in metal−ligand bond covalency and/or (ii) decrease in effective nuclear charge on Eu^{3+} upon complex formation. Malta et al.[15] defined the concept of overlap polarizability of a single directional chemical bond between two atoms A and B, related to the reciprocal of the energy difference between the LUMO and HOMO of AB (taken as the charge transfer energy), the square of the distance between the nuclei, and the squared magnitude of the overlap between the valence shells of A and B. A correlation was given for six solid-state systems doped with Eu^{3+} of E and the sum of overlap polarizabilities of ligating atoms, which was subsequently extended.[16]

The general form of the crystal field Hamiltonian in eq 1, representing nonspherically symmetric interactions between electrons, can be expressed as

$$H_{CF} = \sum_{i=1}^{N} \sum_{k=2,4,6} \sum_{q=-k}^{k} B_q^k C_q^k(i) \quad (7)$$

where the B_q^k (in the following, written as B_{kq}) are the crystal field parameters and the $\mathbf{C}_q^k(i)$ are tensor operators related to the spherical harmonics of rank k and component q; and the sum i is over all electrons of the $4f^N$ configuration. The number of crystal field parameters depends upon the site symmetry of the lanthanide ion, in the present case, Eu^{3+}, ranging from 2 for O_h to 27 for C_1 site symmetry. At the crystalline site, the energy levels of a $^{2S+1}L_J$ multiplet may be split into as many as $2J + 1$ crystal field components for Eu^{3+}, depending upon the site symmetry. These crystal field levels are identified by the irreducible representations (irreps) of the site point group symmetry. In fact, wave functions of different J-multiplets can mix (i.e., J-mixing) when their irreps are the same, as determined by the relevant crystal field parameters. A more concise fashion to express crystal field effects is through the crystal field strength, expressed as

$$N_v = \left[\sum_{k,q} \frac{4\pi}{2k+1}(B_{kq})^2\right]^{1/2} \quad (8)$$

which may include complex components. Specifically, for the second rank crystal field parameters, B_{2q}, the crystal field strength is labeled B_2 in the following.

Hölsä et al.[17] questioned whether the shifts in E for solid-state systems are in fact due to nephelauxetic effects and cited the J-mixing of $^5D_0$. In fact, although the $^5D_0$ intermediate coupling wave function comprises contributions from various singlets, triplets, and septets, J-mixing is relatively unimportant for $^5D_0$ since $^5D_2$ is at rather higher energy. These authors[17] found a linear correlation between E and the cation radius for

dx.doi.org/10.1021/jp400247r | J. Phys. Chem. A 2013, 117, 2771−2781

four Eu^{3+}-doped rare earth oxyhydroxides. Notably, Kushida et al.,[18−22] Dexpert-Ghys et al.,[23] Balda et al.,[24] and Malta et al.[25] have recognized the relationship between the $^7F_1$ splitting, and/or the related B_2 crystal field strength, or B_{20} crystal field parameter, upon the energy E in glasses under site-selective excitation. Tanaka et al.[21] gave the fitted relation

$$E = 6.75 \times 10^{-5} \times {B_{20}}^2 + 17248 \quad (9)$$

for Eu^{3+}-doped $Ca(PO_3)_2$ glass, whereas a linear relation between E and B_2 was reported by Balda et al.[20] for some glasses. These correlations encompassed a wide range of E (from ∼17200 to 17500 cm^{-1}) and were attributed to the J-mixing effect of ^7F_J (J = 2, 4) with $^7F_0$, which serves to push down the $^7F_0$ level. As mentioned above, the energy of the $^5D_0$ state is largely independent of B_2 or B_{20}. A correlation of energy E versus the barycenter of $^7F_2$ has also been given for nanocrystalline Y_2O_3:Eu^{3+}.[26]

The selection rule of J-mixing for a J multiplet with another (J') is determined by the matrix element of the tensor operator in the crystal-field Hamiltonian between angular parts of the free ion wave functions. This matrix element contains a 6j symbol, and for this to be nonzero, the triangle rule $\Delta(J, J', k)$ must be obeyed. For Eu^{3+}, we consider the special case of J = 0, as for $^7F_0$. Hence, for O_h site symmetry of Eu^{3+}, with the crystal field parameters having k = 4 and 6, so J' can take the values of 4 or 6: i.e., $^7F_4$ and $^7F_6$ can mix with $^7F_0$. For C_{3h} symmetry, the nonzero k can be 2, 4, 6, so $^7F_0$ can mix with $^7F_2$, $^7F_4$, and $^7F_6$. For C_{2v} symmetry, the nonzero k can be 2, 4, 6, so $^7F_0$ can also mix with $^7F_2$ $^7F_4$, and $^7F_6$. Even for C_1 site symmetry, the k values of the crystal field Hamiltonian entering into the matrix elements between $4f^6$ states are even due to the parity selection rule, so that $^7F_0$ cannot mix directly with $^7F_1$. However, $^7F_1$ can mix indirectly with $^7F_0$ through $^7F_2$: $^7F_0$−$^7F_2$ (*via* k = 2) and $^7F_2$−$^7F_1$ (via k = 2). The extent of J-mixing is inversely proportional to the energy difference between the J,J'-multiplets. A comprehensive treatment of the J-mixing of $^7F_0$, including the contribution from $^7F_4$, has recently been given.[27]

Therefore, the origin of the shift of the $^5D_0$−$^7F_0$ transition, energy E, in various solid-state systems appears to be controversial. Is it due to a nephelauxetic effect, where the free ion electron repulsion is reduced, or to crystal field effects? Or are these two effects inter-related? Görller-Walrand and Binnemans[28] have stated that there is no correlation between the crystal field parameters and the nephelauxetic effect. The present work aims to provide insight to these questions.

Some calculations have previously been performed to study the variation of E with change in various parameters. When keeping the interelectronic repulsion parameters constant, it was found that an increase in B_{20}, and especially B_{22}, increases E.[29] Variation of the Slater parameters, F^k, showed that an increase in E cannot be associated with an increase in these parameters, but only to a preferential decrease of F^2 with respect to F^4 and F^6.[30,31] All F^k are reduced when the Eu−ligand distance decreases.

THEORETICAL SECTION

The term H_{ADD} in eq 2 is given by

$$H_{ADD} = \alpha \mathbf{L}(\mathbf{L}+1) + \beta G(\mathbf{G_2}) + \gamma G(\mathbf{R}_7) + \sum_s T^s \mathbf{t}_s + \sum_k P^k \mathbf{p}_k + \sum_j M^j \mathbf{m}_j \quad (10)$$

where k = 2, 4, 6; s = 2, 3, 4, 6, 7, 8; j = 0, 2, 4. The two-body configuration interaction parameters α, β, γ parametrize the Coulomb interactions with higher configurations of the same parity, where $G(\mathbf{G_2})$ and $G(\mathbf{R}_7)$ are the eigenvalues of Casimir's operators for the groups $\mathbf{G_2}$ and $\mathbf{R}_7$ used to classify the states of the f^N configuration.[1] The effects of interactions of a configuration of the type l^N, namely f^6, with configurations involving single electron excitation from a closed shell into f^6, or out of f^6 into an unfilled orbital, result in a correction factor to the f^6 configuration where the angular factor of the term describing the interactions involves the coordinates of three electrons.[1] These so-called three-body interactions are parametrized in the effective Hamiltonian by the parameters T^s. The T^s parameters represent the second order refinement of the electron repulsion energies (i.e., splittings of terms) while α, β, γ represent the first order. The magnetic parameters M^j describe the spin−spin and spin−other orbit interactions between electrons, and the electrostatically correlated spin−orbit interaction P^k allows for the effect of additional configurations upon the spin−orbit interaction. All of these parameters fine-tune the free-ion energies.

When there are too many three-particle parameters employed in the fit, their values cannot be reliably determined and so they will be largely affected by errors in some term energies. For the Eu^{3+} energy levels, we cannot say that the T^2 value from any system is reliable unless there are experimental data of energy levels for more than 12 different LS terms found in that system.

However, the value of the three-body parameter T^2 affects the fitted values of the Slater parameters F^k, so that it is necessary to correct these fitted values. According to Judd,[32] the three-particle operator $\mathbf{t}_2$ can be decomposed into the components following eq 9 of ref 32:

$$\mathbf{t}_2 = \frac{8\mathbf{t}_2' - 3\mathbf{t}_2''}{1400\sqrt{2}} + \frac{(N-2)\mathbf{e}_3}{70\sqrt{2}} \quad (11)$$

where N is the number of 4f electrons (for Eu^{3+}, N = 6) and $\mathbf{e}_3$ is the two-particle Racah operator:

$$\mathbf{e}_3 = \frac{75 \times 11}{14}\mathbf{f}_2 + \frac{4 \times 99}{7}\mathbf{f}_4 - \frac{5577}{25 \times 2}\mathbf{f}_6 \quad (12)$$

Hence, the fitted values of the Slater parameters F^k should be corrected by the following equation:

$$\sum_k F^k \mathbf{f}_k \rightarrow \sum_k (F^k + \Delta F^k)\mathbf{f}_k = \sum_k F^k \mathbf{f}_k + T^2 \frac{(N-2)\mathbf{e}_3}{70\sqrt{2}} \quad (13)$$

i.e.,

$$\sum_k \Delta F^k \mathbf{f}_k = T^2 \frac{(N-2)}{70\sqrt{2}} \left\{ \frac{75 \times 11}{14}\mathbf{f}_2 + \frac{4 \times 99}{7}\mathbf{f}_4 - \frac{5577}{25 \times 2}\mathbf{f}_6 \right\} \quad (14)$$

Numerically,

$$\Delta F^2 = 0.5953(N-2)T^2, \quad \Delta F^4 = 0.5715(N-2)T^2, \quad \text{and} \quad \Delta F^6 = -1.127(N-2)T^2 \quad (15)$$

This equation is consistent with the linear dependence on N as shown in eqs 5−7) of ref 33.

dx.doi.org/10.1021/jp400247r | J. Phys. Chem. A 2013, 117, 2771−2781

RESULTS AND DISCUSSION

Relation between E and $^7F_1$ Splitting in Eu^{3+}-Doped Lead Borate Glass. Kushida et al. investigated the effects of the crystalline field upon the $^5D_0$–$^7F_0$ energy, E, in various glasses.[18−22] The site symmetry of Eu^{3+} in glasses may be as low as C_1, but has often been modeled by C_2 or C_{2v} to avoid excessive parametrization. By employing the pure Russell–Saunders states ^7F_J and $^5D_0$, when considering the J-mixing of $^7F_1$ with $^7F_2$ and $^7F_3$, and the mixing of $^7F_2$ with $^7F_0$, it was found that

1. The energy splitting of $^7F_1$ is proportional to B_{20} and B_{22}.
2. The mean energy of the three $^7F_1$ levels, $E(^7F_1)$, is given by

$$E(^7F_1) = (7\beta + 2\gamma/\alpha)\{E(^7F_0) - E_0(^7F_0)\} + E_0(^7F_1) \quad (16)$$

where the $E_0(^7F_0)$ and $E_0(^7F_1)$ energies referred to $B_{2q} = 0$, and α, β, γ are J-mixing coefficients.[20] Making the further assumption that the energy of $^5D_0$ is independent of the ion site, then the plot of $E(^7F_1)$ versus E should be linear with the slope of $(7\beta + 2\gamma/\alpha)$. The approximations implicit in this value are that J-mixing of $^7F_0$ with $^7F_4$ is not included, in addition to all other interactions of $^7F_0$ with other multiplets. The reader is referred to ref 20 for further details. The arguments imply that $^7F_0$ is pushed downward by J-mixing with $^7F_2$, while $^7F_1$ is pushed down by J-mixing with $^7F_2$ and $^7F_3$. We demonstrate agreement and the validity of these assumptions by utilizing data from the lead borate glasses $(B_2O_3)_z(PbO)_{99.6-z}(0.5Eu_2O_3)_{0.4}$ for various values of z, and for different excitation wavelengths into $^5D_2$. The emission spectra have previously been published in ref 34, Figures 4 and 5. Figure 1a shows the plot of $E(^7F_1)$ vs E from Figure 4,[34] i.e., the mean value of the three $^5D_0 \rightarrow {}^7F_1$ emission lines is plotted against the $^5D_0 \rightarrow {}^7F_0$ energy for glasses with the compositions z = 20, 30, 40, 60, 70. The slope is 0.63 ± 0.05, which is reasonable considering the approximations in the value of $(7\beta + 2\gamma/\alpha) \sim 0.55$ from our spectral measurements. Figures 1b,c show plots for one glass (z = 60) using different excitation lines into $^5D_0 \rightarrow {}^7F_2$. Figure 1b depicts the splitting of the $^7F_1$ multiplet for these different excitation wavelengths, versus the $^5D_0 \rightarrow {}^7F_0$ energy, E, in each case. The change in $^7F_1$ splitting, by more than a factor of 3 in this figure, is clearly a crystal field effect and is not related to changes in Slater parameters or spin–orbit coupling. The $^7F_1$ splitting is linearly related to E. The excitation energy is compared with the energy E in Figure 1c. Since the major shifts of $^7F_0$–$^5D_0$ and $^7F_0$–$^5D_2$ arise from the depression of $^7F_0$, both $^5D_0$ and $^5D_2$ behave in a fairly similar fashion.

Literature Data for E, B_2, and $^7F_1$ Splitting. Plentiful literature data are available from the $^5D_0$ luminescence spectra of solid-state systems doped with Eu^{3+}, notably at 77–10 K. We have selected the spectra of Eu^{3+} doped into well-characterized host lattices, with oxygen coordination, and in order to further examine the crystal field effects upon the $^7F_1$ levels and the $^5D_0$–$^7F_0$ energy, only those data were selected for systems with Eu^{3+} site symmetry of C_{2v}, C_2, C_s, and C_1. Figure 2a shows the linear relation between the second rank crystal field strength and the $^7F_1$ splitting from the data of 58 spectra. The entire low symmetry oxide data set from 112 spectra was employed for the plot of $^5D_0$–$^7F_0$ energy, E, versus $^7F_1$ splitting, Figure 2b, whereas the subset with coordination number 7, Figure 2c, provides a higher coefficient of determination for the same plot but gives the same slope. Both plots indicate strong and

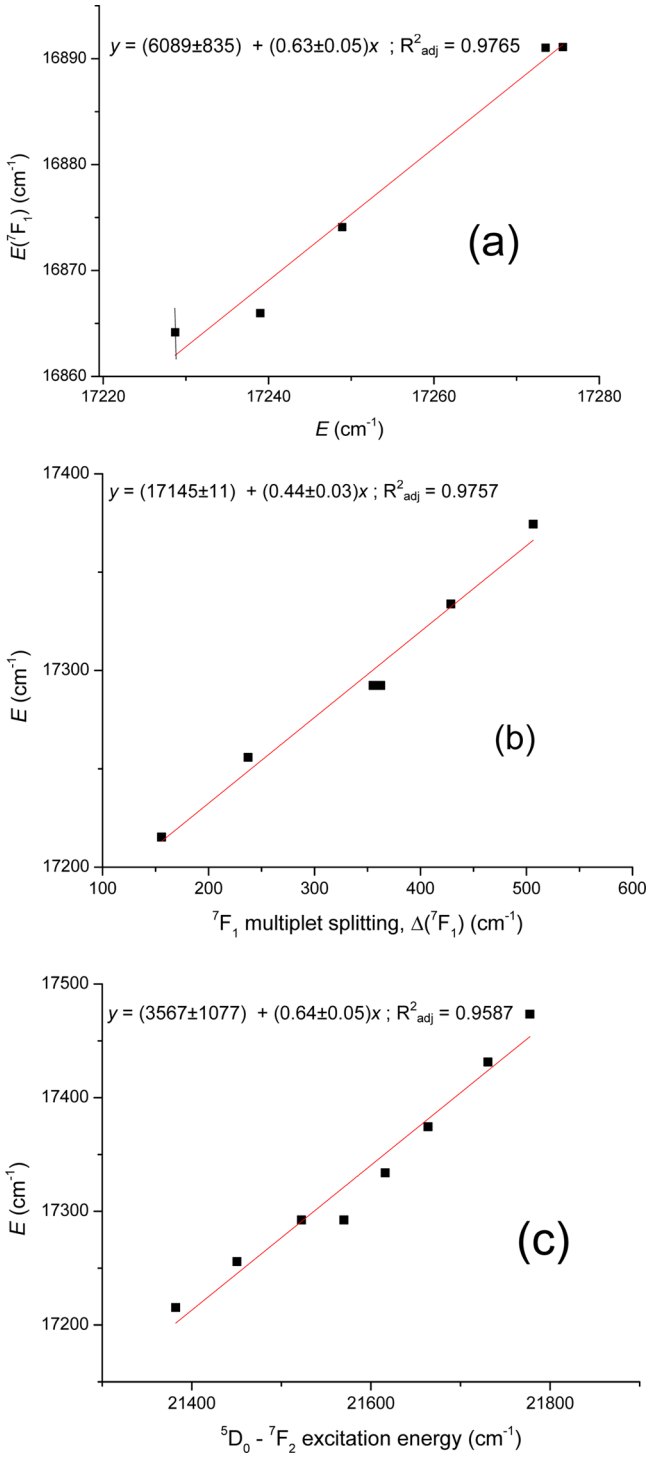

Figure 1. Data from lead borate glasses $(B_2O_3)_z(PbO)_{99.6-z}(0.5Eu_2O_3)_{0.4}$ for various values of z, and for different excitation wavelengths into $^5D_2$.[34] (a) Plot of $E(^7F_1)$ vs E for glasses with the compositions z = 20, 30, 40, 60, 70. (b, c) Plots for the glass z = 60: (b) E vs $\Delta(^7F_1)$; (c) E vs λ_{exc}.

significant relationships between the variables. These experimental results emphasize the role of the crystal field, rather than electron–electron repulsion, in tuning the energy E for other low symmetry systems besides glasses.

The relationship between the $^7F_1$ splitting and E was explored for 41 stoichiometric europium compounds, mostly with oxygen ligands, and the adjusted coefficient of

dx.doi.org/10.1021/jp400247r | J. Phys. Chem. A 2013, 117, 2771–2781

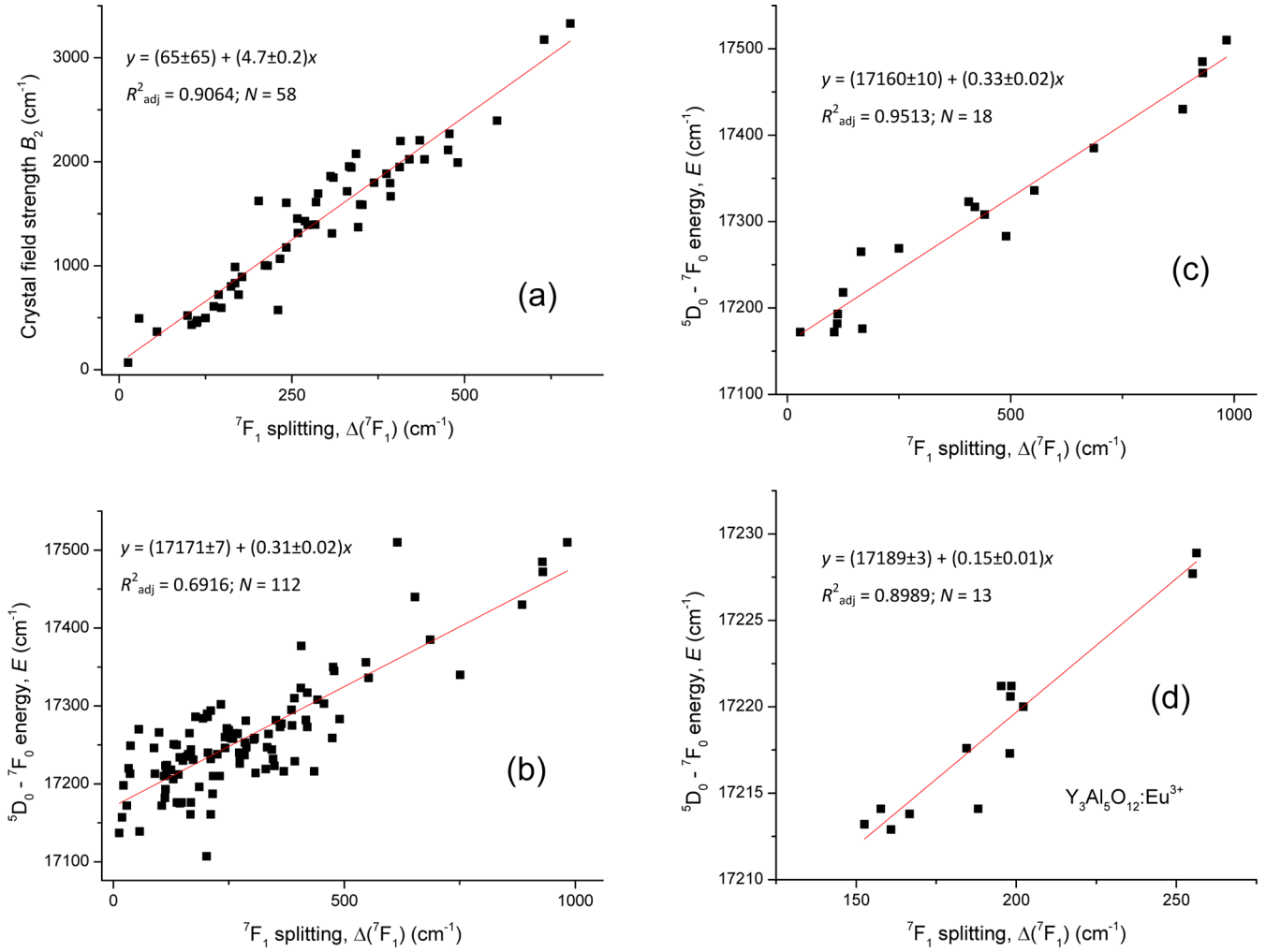

Figure 2. Solid-state spectra of low symmetry oxide systems doped with Eu^{3+}: (a) B_2 vs Δ($^7F_1$); (b) E vs Δ($^7F_1$) for data set; (c) E vs Δ($^7F_1$) for 7-coordinate systems; (d) E vs Δ($^7F_1$) for YAG:Eu^{3+}.

determination was found to be 0.2180. When the data set was reduced to compounds with C_1, C_2, C_s, or C_{2v} symmetry, R_{adj}^2 increased to 0.3483 for 26 compounds. The crystal field splitting of $^7F_1$ alone cannot therefore provide a good explanation of the variance of E in these compounds although the relation is significant at the 0.001 level for the low symmetry systems.

Finally, the variation of $^5D_0$–$^7F_0$ energy was investigated for one specific oxide system. Shen et al.[35] investigated the 12 K site-selective excitation spectra of $Y_3Al_5O_{12}$:Eu^{3+} and identified many centers where Eu^{3+} is situated at perturbed sites. Some of local site structures were identified. The regular, unperturbed Eu^{3+} site symmetry is D_2. Figure 2d shows the relationship between E and the $^7F_1$ splitting for the unperturbed and perturbed sites, and a similar plot results if B_2 instead of Δ($^7F_1$) is employed. The change in E is mainly due to crystal field effects rather than interelectronic repulsion effects.

Model Calculations of the Variation of $^5D_0$–$^7F_0$ Energy. A computational investigation is given in this section of the effects of changing various energy parameters upon the $^5D_0$ energy.

It has been pointed out previously that calculations of the $4f^6$ energy levels which utilize only the F and D terms can provide reasonably accurate crystal field splittings, except for ^5D_J, but the free ion parameters are not well-defined.[29,36] Many years ago, Wybourne[1] also stressed that, in order to derive accurate parameters from experimental energy level data, it is essential that the data contain several different terms of the configuration. Therefore our energy level simulations have included the complete 3003 states of $4f^6$, with the inclusion of the spin–spin interactions (eq 10 in the free ion Hamiltonian).[37] Our experimental energy level data sets have been restricted to those comprising the most terms.

First, the scenario with high symmetry for Eu^{3+} was investigated. In $Cs_2NaEuCl_6$, (Figure 3a), Eu^{3+} is six-coordinated to Cl^- at a site of O_h symmetry. The J-mixing of $^7F_0$ is limited to that with $^7F_4$ and $^7F_6$, and since the relevant states of these multiplets are at relatively high energy (>3000

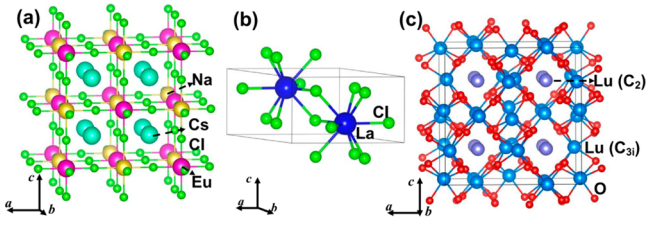

Figure 3. Crystal structures of $Cs_2NaEuCl_6$ (a), $LaCl_3$ (b), and Lu_2O_3 (c).

dx.doi.org/10.1021/jp400247r | J. Phys. Chem. A 2013, 117, 2771–2781

Table 1. Calculated $^7F_1$ and $^5D_0$ Energy Levels (in cm^{-1}) for $Cs_2NaEuCl_6$ and $LaCl_3$:Eu^{3+} When Increasing Absolute Parameter Values by 10%

		calcd energy							
		$Cs_2NaEuCl_6$				$LaCl_3$:Eu^{3+}			
param	value	$^7F_1$	$^5D_0$	$^5D_0$ F.I.[a]	$^5D_0$ F.I.[b]	$^7F_1$	$^5D_0$	$^5D_0$ F.I.[a]	$^5D_0$ F.I.[b]
	fitted	369	17213	17192	17223	365,416	17275	17277	17273
F^2	+10%	374	16958	16936	16969	370,421	17022	17024	17021
F^4	+10%	359	18198	18177	18208	354,406	18225	18228	18223
F^6	+10%	350	18488	18467	18498	345,397	18561	18564	18559
F^k	+10%	345	19258	19234	19269	340,392	19297	19299	19295
$\zeta(4f)$	+10%	441	16888	16871	16895	437,488	16955	16959	16953
α	+10%	369	17199	17179	17210	365,417	17261	17264	17259
$\lvert\beta\rvert$[c]	+10%	370	17145	17124	17155	366,417	17212	17215	17210
γ	+10%	367	17349	17329	17359	363,414	17439	17441	17441
α, $\lvert\beta\rvert$,[c] γ	+10%	369	17268	17247	17278	364,415	17362	17365	17361
T^2	+10%	370	17166	17145	17176	366,417	17218	17221	17216
T^3	+10%	369	17213	17192	17223	365,416	17275	17277	17277
T^4	+10%	369	17211	17190	17221	365,416	17273	17276	17271
$\lvert T^6\rvert$[c]	+10%	369	17212	17191	17222	365,416	17274	17277	17272
T^7	+10%	369	17211	17191	17221	365,416	17272	17275	17270
T^8	+10%	369	17224	17203	17234	364,416	17292	17295	17290
$\lvert T^k\rvert$[c]	+10%	370	17173	17153	17183	366,417	17228	17230	17226
M^k	+10%	368	17206	17185	17216	364,416	17268	17271	17266
P^k	+10%	370	17216	17195	17226	365,416	17276	17279	17274
B_{20}	+10%					363,420	17275	17277	17273
$\lvert B_{40}\rvert$	+10%	367	17217	17192	17230	[c]365,416	17275	17277	17273
$\lvert B_{60}\rvert$	+10%	369	17212	17192	17222	[c]365,417	17274	17277	17272
B_{66}	+10%					365,416	17274	17277	17272

[a] $B_{kq} = 0$. [b] $B_{kq} \neq 0$. [c] These parameters have negative values.

Table 2. Shift in Calculated Values of Some Energy Levels of Lu_2O_3:Eu^{3+} (in cm^{-1}) for 10% or 200% Increase in the Rank Two Crystal Field Parameters

	fitted value	+10% in $\lvert B_{20}\rvert$	+10% in $\lvert B_{22}\rvert$	+10% in $\lvert B_{20}\rvert$ and $\lvert B_{22}\rvert$	+200% in $\lvert B_{20}\rvert$	+200% in $\lvert B_{22}\rvert$
B_{20}	−270	−297	−270	−297	−809	−270
B_{22}	−757	−757	−833	−833	−757	−2272
$^7F_0$	−7	−7	−19	−18	−9	−330
$^7F_1$	210, 364, 559	212, 360, 560	185, 358, 565	189, 356, 568	256, 285, 584	−252, 184, 392
$\Delta(^7F_1)$	349	348	380	379	328	644
$^5D_0$	17213	17212	17212	17213	17214	17237
E	17220	17219	17231	17231	17223	17567

cm^{-1}), this case represents minimal J-mixing so that a clear picture of the effects in changing free ion parameters upon energy E can be obtained. In line 3, columns 3 and 4, Table 1, the energies of the triply degenerate $^7F_1$ and nondegenerate $^5D_0$ states are listed, from a fit to 77 experimental energy levels, with some of the parameter values subsequently discussed and listed in Table 3 and Table S1 in the Supporting Information. In both cases, the $^7F_0$ energy is placed at 0 cm^{-1}, so that the $^5D_0$ energy equals E. The new values resulting from the effects of increasing the parameter absolute values by 10% are listed below the fitted values. There is a decrease in E of 255 cm^{-1} for the F^2 increase, whereas increases in F^4 and F^6 lead to increases in E of 985 cm^{-1} and 1275 cm^{-1}, respectively. These changes result from the changes in interelectronic repulsion, and the combined increase of F^2, F^4, and F^6 each by 10% leads to an increase in E by 2045 cm^{-1}, which is slightly larger than the sum of the individual increases. The increase in the spin−orbit coupling constant by 10% provides a decrease in E of 325 cm^{-1}. The changes in E were found to be linearly related to individual changes in F^2, F^4, F^6, or ζ_f. These represent the major changes in E for changes in all of the parameter values. Notably, the 10% increase in the fourth- or sixth-rank crystal field parameters leaves the energies of $^7F_1$ and $^5D_0$ virtually unchanged. The $^5D_0$ energies in column 4 represent the free ion energies, whereas those in column 5 are free ion energies with the crystal field J-mixing effect included. Values in column 4 show a fairly constant decrease by ∼21 cm^{-1} of those in column 3, whereas the column 5 energies are ∼10 cm^{-1} higher than the column 3 energies.

An analogous calculation was performed by fitting 60 energy levels of $LaCl_3$:Eu^{3+} (Refer to Table 1, columns 7−10, Table 3, and Table S1 in the Supporting Information), where Eu^{3+} is situated at a site of C_{3h} symmetry, surrounded by 3 Cl^- in the same mirror plane, and by two sets of 3 Cl^- above and below which define a triangular prism about Eu^{3+} (Figure 3b).[38] It is well-known that nine coordination of Eu^{3+} (C_{3h} or D_{3h} symmetry point group) produces a weak crystal field and that J-mixing is relatively unimportant.[39] Thus, the energy changes in E resulting from 10% increase of F^2, F^4, F^6, or ζ_f are very similar to those given above, as are the energy changes of $^7F_1$. It

dx.doi.org/10.1021/jp400247r | J. Phys. Chem. A 2013, 117, 2771−2781

Table 3. Parameter Values (cm^{-1}) from Energy Level Calculations of Eu^{3+} Systems[a]

label	system	moiety, site	ref	N_{expt}	F^2	F^4	F^6	ζ_f	E(expt)	B_2	T^2
1a	Cs_2NaYF_6	EuF_6, O_h	this work	59	81978 ± 416	61402 ± 454	42625 ± 189	1321.7 ± 1.8		0	227
					82519 ± 471	*61921 ± 507*	*41602 ± 293*				
1b	Cs_2NaYF_6	EuF_6, O_h	40	57	86460	62286	29844	1347	17255	0	−2987
					79348	*55458*	*43306*				
1c	Cs_2NaYF_6	EuF_6, O_h	41	21	83789 ± 50	[59909]	[41308]	1323 ± 13	17255	0	370
					84670	*60755*	*39640*				
2	$LiYF_4$	EuF_8, S_4	42	103	82210 ± 9	59154 ± 19	43090 ± 11	1330 ± 1	17270	349	349
					83091 ± 16	*60000 ± 26*	*41422 ± 25*				
3a	Lu_2O_3	EuO_6, C_2	43	105	81098 ± 35	58141 ± 53	43085 ± 48	1335 ± 5	17216	1798	370
					81979	*58987*	*41417*				
3b	Lu_2O_3	EuO_6, C_2	this work	126	81569 ± 84	57419 ± 202	45171 ± 326	1335.5 ± 0.8		1752	772
					83407 ± 258	*59184 ± 369*	*41692 ± 655*				
4	In_2O_3	EuO_6, C_2	44	48	80206 ± 108	59968 ± 774	41068 ± 465	1313 ± 3	17229	1668	300
					80920	*60654*	*39716*				
5	$Y_3Ga_5O_{12}$	EuO_8, D_2	45	73	82347 ± 57	59844 ± 69	42359 ± 43	1333.8 ± 1.8	17210	349	416
					83338 ± 69	*60795 ± 80*	*40484 ± 66*				
6	$Y_3Al_5O_{12}$	EuO_8, D_2	46	90	82764 ± 64	59389 ± 374	42641 ± 195	1333.2 ± 1.5	17207	761	416
					83755 ± 102	*60340 ± 411*	*40766 ± 267*				
7a	TiO_2	C_{2v}	27	47	82256	61248	40411	1324	17107	1624	n.a.
7b	TiO_2	D_2	27	42	84685	60381	41288	1349	17063	1001	n.a.
8	$Na_3[Yb(dpa)_3]$ $NaClO_4{\cdot}10H_2O$	EuO_6N_3, D_3	47	52	82468 ± 58	59150 ± 79	43116 ± 47	1336 ± 1	17191	431	370
					83349	*59996*	*41448*				
9	$Eu(DBM)_3{\cdot}H_2O$	EuO_7, C_3	48	74	83025	61202	41520	1326	17243	812	n.a.
10	$Eu_2Zn_3(NO_3)_{12}{\cdot}24H_2O$	EuO_{12}, C_{3v}	49	40	81333 ± 84	58267 ± 27	43288	1348 ± 1	17247	243	330
					82119	*59021*	*41801*				
11	$GdAl_3(BO_3)_4$	EuO_6, D_3	50	68	81787 ± 60	59534 ± 71	43017 ± 40	1328.9 ± 1.2	17245	840	415
					82775 ± 89	*60483 ± 98*	*41147 ± 94*				
12	$Eu(C_2H_5SO_4)_3{\cdot}9H_2O$	EuO_9,C_{3h}	51	78	82969	60185	43448	1342	17256	266	330
					83755	*60939*	*41961*				
13	$Na_3[Eu(ODA)_3]$ $2NaClO_4{\cdot}6H_2O$	EuO_9,D_3	52	61	82458 ± 26	59293 ± 40	43112 ± 41	1332 ± 4	17231	65	370
					83339	*60139*	*41444*				
14	$Eu[(CH_3COO)_3$ $(H_2O)_2]_2{\cdot}H_2O$	EuO_9,C_1	53	130	82623 ± 14	59428 ± 31	42968 ± 29	1335 ± 1	17239	247	370
					83504	*60274*	*41300*				
15	$EuCl_3{\cdot}6H_2O$	EuO_6Cl_2, C_2	54	58	82031 ± 254	59233 ± 194	42729 ± 214	1336.8 ± 1.5	17269	517	376
					82926 ± 287	*60093 ± 226*	*41034 ± 277*				
16a	$LaCl_3$	$EuCl_9$, C_{3h}	55	58	84374 ± 35	60188 ± 45	41658 ± 35	1330 ± 2	17267.4	419	370
					85255 ± 35	*61034 ± 45*	*39990 ± 35*				
16b	$LaCl_3$	$EuCl_9$, C_{3h}	this work	60	78011 ± 146	57063 ± 47	44286 ± 67	1344.2 ± 0.4		282	633
					79518 ± 189	*58510 ± 88*	*41433 ± 148*				
17a	$Cs_2NaEuCl_6$	$EuCl_6$, O_h	this work	77	80504 ± 296	60184 ± 420	42210 ± 287	1324.7 ± 1.4		0	339
					81311 ± 360	*60959 ± 482*	*40682 ± 409*				
17b	$Cs_2NaEuCl_6$	$EuCl_6$, O_h	33	77	79688 ± 109	61547 ± 229	43044 ± 141	1331 ± 2	17208	0	278
					80350 ± 128	*62183 ± 247*	*41791 ± 177*				

dx.doi.org/10.1021/jp400247r | J. Phys. Chem. A 2013, 117, 2771−2781

Table 3. continued

label	system	moiety, site	ref	N_{expt}	F^2	F^4	F^6	ζ_f	E(expt)	B_2	T^2
17c	$Cs_2NaEuCl_6$	$EuCl_6$, O_h	40	77	94613	87348	51081	1342	17208	0	−256
					94003	*86763*	*52235*				
A	$(Eu-F)_{av}$ $N = 2$				82094 ± 164	60278 ± 1590	42858 ± 329	1326 ± 9	17263 ± 11		
					82805 ± 404	*60961 ± 1358*	*41512 ± 127*				
B	$(Eu-O)_{av}$ $N = 9$				82319 ± 617	59396 ± 1078	43058 ± 982	1334 ± 11	17233 ± 18		
	$N = 8$				*83249 ± 550*	*60147 ± 698*	*41324 ± 512*				
C	$(Eu-Cl)_{av}$ $N = 2$				79258 ± 1763	58624 ± 2207	43248 ± 1468	1335 ± 14	17238 ± 42		
					80415 ± 1268	*59735 ± 1732*	*41058 ± 531*				

[a]Values in square brackets were constrained. dpa =2,6-pyridinedicarboxylato; ODA = oxydiacetato; DBM = dibenzoylmethanato; row A comprises average values from rows 1a, 2; row B (top) comprises the average of 3b, 5, 6, 9, 10, 11, 12,13, 14; row B bottom omits row 9. The average values from rows 16b, 17a are displayed in row C.

has been shown previously that the $^7F_1$ splitting is linearly proportional to the crystal field parameter B_{20} for hexagonal, tetragonal, or trigonal crystal fields (ref 28, page 222). Hence the 10% increase in B_{20} for $LaCl_3:Eu^{3+}$ produces a similar increase in the $^7F_1$ splitting (Table 1).

In summary, the values of E for these two systems are most sensitive to changes in Slater parameters and the spin−orbit coupling constant. The changes are not all in the same direction, and those from F^4 and F^6 are relatively greatest. These two systems represent cases of fairly high symmetry so that the J-mixing of $^7F_0$ is not of major importance.

It is instructive to examine the crystal field effect in lower symmetry. In the Lu_2O_3 crystal, one of the sites occupied by Eu^{3+} has C_2 symmetry. The Eu^{3+} ion is situated by six O^{2-} at the corners of a cube, with two missing from the diagonal of one face (Figure 3c). A preliminary calculation was performed by fitting 105 levels, and the items of interest are collected in Table 2, columns 1, 2. Here, the values of B_{20} and the real parameter B_{22}, together with the $^7F_1$ splitting, $\Delta(^7F_1)$, the calculated values of $^7F_0$ and $^5D_0$, and the energy difference, E, are listed. The effects of increasing the crystal field parameters individually, or jointly, by 10% or 200% are subsequently given in the table. Multiplying $|B_{22}|$ by a factor of 3 produces the result that the $^5D_0-^7F_0$ energy is at 17567 cm^{-1} and the $^7F_1$ splitting is 644 cm^{-1}, implying a slope of ∼0.5, which is comparable with that in Figure 1b of 0.5, and can provide an explanation for these extreme values via crystal field interactions. It is interesting that, in the case of Lu_2O_3, it is the change in B_{22} and not B_{20} that provides the greatest crystal field perturbation.

Mechanisms for Shift of $^5D_0-^7F_0$ Energy. The above results show that there are several distinct reasons for the shifts in E in different Eu^{3+} systems. The physical mechanisms are now described for each case, starting with the shifts due to crystal field J-mixing in low symmetry systems.

It is instructive to examine the composition of the ground state and $^5D_0$ wave functions to assess the extent of J-mixing. The "best-fit" calculation for $Lu_2O_3:Eu^{3+}$ gives the leading components of the $^7F_0$ wave function $|^{2S+1}L\ J\ M_J\rangle$, comprising real and complex components:

$$85.5\%|^7F\ 0\ 0\rangle + 3.0\%|^5D(1)\ 0\ 0\rangle + 2.7\%|^7F\ 2\ 2\rangle + 2.7\%\ |^7F\ 2\ -2\rangle + 2.6\%|^5D(3)\ 0\ 0\rangle$$

(where the two numbers after the term represent J and M_J values) indicating some J-mixing of $^7F_0$ with $^7F_2$ induced by the $k = 2$, 4 rank crystal field parameters.

With the 200% increase in B_{22}, the wave function becomes

$$65.2\%|^7F\ 0\ 0\rangle + 12.2\%|^7F\ 2\ 2\rangle + 12.2\%|^7F\ 2\ -2\rangle + 2.4\%\ |^5D(1)\ 0\ 0\rangle + 1.9\%|^5D(3)\ 0\ 0\rangle$$

showing a considerable increase in the $^7F_2$ components through J-mixing by B_{22}. By contrast, even with the 200% increase in B_{22}, the wave function of $^5D(3)_0$ is

$$45.8\%|^5D(3)\ 0\ 0\rangle + 28.9\%|^5D(1)\ 0\ 0\rangle + 6.2\%|^3P(6)00\rangle + 6.0\%|^7F\ 0\ 0\rangle + 4.8\%|^3P(3)\ 0\ 0\rangle$$

and comprises only $J = 0$ components, so that J-mixing is unimportant for $^5D_0$. From the results for Eu^{3+} doped into glasses and low symmetry systems it is evident that J-mixing contributes to the largest shifts for the $^5D_0-^7F_0$ energy.

However, the intricate free ion mixing of $^5D(3)$ is also responsible for shifting E, as described now for the system $Cs_2NaEuCl_6$ where J-mixing is unimportant.

The changes in E for the high symmetry system $Cs_2NaEuCl_6$ resulting from changes in interelectronic repulsion are a consequence of the free ion mixing of $^5D(i)_0$ (i = 1−3) multiplets. In this system, the $^5D(3)_0$ J-multiplet of Eu^{3+} is mixed up with the $^5D(1)_0$, $^3P(6)_0$, and $^7F_0$ multiplets as follows:

$$46.3\%|^5D(3)_0\rangle + 29.1\%|^5D(1)_0\rangle + 6.3\%|^3P(6)_0\rangle + 5.9\%|^7F_0\rangle$$

The reduced matrix element (RME) between $^5D(3)$ and $^5D(1)$ is 0.273, 0.0677, and −0.1518 for the operator $\mathbf{f}_2$, $\mathbf{f}_4$, and $\mathbf{f}_6$, respectively. The RME between $^5D(3)$ and other relevant terms is zero, and the RME of the diagonal terms all have the same sign and comparable magnitude for all the $\mathbf{f}_k$ operators. Hence, the likely reason for the decreasing effect of F^2 on the $^5D(3)$ term (including all J = 0−4 multiplets) is that the effect of term mixing between $^5D(3)$ and $^5D(1)$ pushes one term $^5D(3)$ downward and offsets the increase in the diagonal term of the $\mathbf{f}_2$ operator, while the other term $^5D(1)$ is pushed in the opposite direction. For example, in $Cs_2NaEuCl_6$, $E(^5D(1)_0)$ is calculated to change from 74222 cm^{-1} to 79891 cm^{-1} when F^2 increases by 10%; or to 75985 cm^{-1} when F^4 increases by 10%; or to 75014 cm^{-1} when F^6 increases by 10%.

The other major reason for shifts in E in different Eu^{3+} systems is due to changes in the magnitude of spin−orbit splitting within the term $^5D(3)$. When ζ_f is increased for Eu^{3+} in $Cs_2NaEuCl_6$, the spin−orbit splitting is enhanced (from $E(^5D(3)_4) - E(^5D(3)_0)$ = 10367 cm^{-1} to 11336 cm^{-1} for a 10% increase in ζ_f) in which the lower J-multiplets (J = 0 and 1) will be pushed downward while the upper J-multiplets will be pushed further upward. The same phenomena happen in the ground ^7F term, where the magnitude of the spin−orbit splitting is increased from 4968 cm^{-1} to 5545 cm^{-1}, but this is not as large an effect as for the magnitude for the $^5D(3)$ term. Overall, the $^5D(3)_0$ multiplet is moved downward relative to $^7F_0$, while $^7F_0$ actually also moves downward but not to the same large extent.

Energy Level Data Sets for Eu^{3+} in Solid-State Systems. A literature search showed that very few crystal field calculations of Eu^{3+} have extended beyond the F and D terms, so that only in those cases can the Slater parameters be more accurately determined. Some calculations which have utilized more extended energy level data sets are listed in Table 3, with the coordination environment and site symmetry of Eu^{3+} identified. In most cases, use has been made of the polarization of spectral features, and in several, Zeeman studies have been employed. Only one or two additional terms to D and F were included for In_2O_3 and TiO_2, and the spectral assignments are arbitrary in many cases for Lu_2O_3 and $Eu[(CH_3COO)_3(H_2O)_2]_2(H_2O)$. The calculated Slater parameters, spin−orbit coupling constant, and second rank crystal field strength (if applicable) are also given at the top of each row, together with the number, N_{expt}, of energy levels fitted, and the $^5D_0$−$^7F_0$ energy, E. As mentioned above, some parameter values are not mutually independent. For example F^2 is correlated with T^2 so that an erroneous T^2 value produces a consequential error in F^2. The T^2 values, where available, are listed in the final column of Table 3. We observed that several parameter values in Table 3 did appear to be anomalous, for example, F^6 in row 1b; ζ_f in 1b, 4, 7b, 17c; F^2, F^4, F^6 in 17c. We have repeated some calculations, as indicated (rows 1a, 3b, 16b, 17a). In each case, except for row 17b, we were unable to replicate the previous calculation so that the revised values from our calculations are also listed in these rows. It is out of the scope of this work to repeat all of these calculations, but we note that errors in matrix elements of such calculations have persisted in some cases up to 2008,[56] and spin−spin interactions have only been included in our calculations.[37] The parameter values and descriptions of the data sets employed in our revised calculations are included in the Supporting Information.

First, the effects of the ligand upon the Slater and spin−orbit coupling parameters are considered, since these are the prime indicators of nephelauxetic effects. The corrected Slater parameters for each system are listed in italics underneath the reported or fitted values. It is evident from the table that individual parameter values for a given ligand type exhibit a wide variation compared with the respective parameter values for different types of ligands. The available mean values for F, O, and Cl ligands are collected at the bottom of Table 3: rows A−C. The mean corrected F^k values of chloride systems are 1−3% smaller for those for fluoride systems, but data for only two systems are available in each case, the values differ by only one standard deviation, and there are individual exceptions to these conclusions. The mean fluoride spin−orbit coupling constant is 0.7% lower than the mean value for the chloride systems, but again the values for all systems lie within a standard deviation. The mean F^k values for oxide systems (Table 3, row B) are closer to those for fluorides, whereas the magnitude of the spin−orbit coupling constant is nearer to the value for chlorides. Within the precision of the present data, there are no overall clear distinctions of nephelauxetic effects for fluorides, oxides, and chlorides. The mean ratios of fitted F^4/F^2 and F^6/F^2 from the values in rows A, B, C of Table 3 are 0.73 ± 0.01 and 0.53 ± 0.01, respectively, which are both higher than the hydrogenic ratios of 0.668 and 0.494.

There are no simple relationships between E and the ligand type, or the coordination number of Eu^{3+}, in Table 3, or from the literature data for solid-state systems that we collected. Also, the simple relationship of E with second rank crystal field strength, B_2, is not observed in Table 3 because many systems have Eu^{3+} situated at sites of relatively high symmetry. For the octahedral systems, the values of E are (in cm^{-1}) 17255 for EuF_6^{3-} and 17208 for $EuCl_6^{3-}$, but available data for $EuBr_6^{3-}$ (17217 in $Cs_2NaLuBr_6$:Eu^{3+})[57] and EuO_6^{9-} (17137 in Ba_2YNbO_6)[58] do not follow an expected trend.

CONCLUSIONS

Experimental energy level data are lacking for Eu^{3+} due to the extended nature of the $4f^6$ configuration, which overlaps $4f^55d^1$. For example, the $^5D(1)_J$ multiplets have not been identified. Hence at present, the Slater parameters and spin−orbit coupling constants available from data set fittings do not enable clear conclusions to be made concerning nephelauxetic trends. However it does appear that such trends involve small changes and that they may be masked by other effects, such as changes in site symmetry. A lanthanide ion such as Pr^{3+}, where all of the terms have been experimentally located in some solid-state systems, three-body parameters are absent from the Hamiltonian, and the Slater parameters are more accurately determined, may give a more accurate indication of the importance of nephelauxetic effects in relation to atomic energy parameters. This will be investigated by us in the future.

dx.doi.org/10.1021/jp400247r | J. Phys. Chem. A 2013, 117, 2771−2781

The variation of the $^5D_0-^7F_0$ energy, E, in Eu^{3+} systems cannot be represented by a simple relationship because it is affected by several factors. The largest variations in E occur for low symmetry systems, and the mechanism has been identified as the depression of $^7F_0$ due to direct crystal field J-mixing with ^7F_J (J = 2,4,6), with J = 2 being most important, and indirect mixing with J = 1. The most important other mechanisms which provide changes in E are due to changes in Slater parameters and the spin−orbit coupling constant, although these changes are not all in the same direction.

■ ASSOCIATED CONTENT

Supporting Information

Description of ^5D states; parameter values for best fit energy level calculations; comments upon energy level data fits. This material is available free of charge via the Internet at http://pubs.acs.org.

■ AUTHOR INFORMATION

Notes

The authors declare no competing financial interest.

■ ACKNOWLEDGMENTS

We are very grateful to the HKIEd for various kinds of financial support in this research, including the provision of the Visiting Professorship to P.A.T. L.N. gratefully acknowledges the financial support from the National Science Foundation of China (Grant No. 11174005).

■ REFERENCES

(1) Wybourne, B. G. *Spectroscopic Properties of Rare Earths*; Interscience: London, 1965; p 44.
(2) Jørgensen, C. K. The Nephelauxetic Series. *Progress in Inorganic Chemistry*; Cotton, F. A., Ed.; Wiley: New York, 1962; Vol. *4*, p 73−124.
(3) Newman, D. J. Ligand Ordering Parameters. *Aust. J. Phys.* **1977**, *30*, 315−323.
(4) Schäffer, C. E.; Jørgensen, C. K. The Nephelauxetic Series of Ligands. *J. Inorg. Nucl. Chem.* **1958**, *8*, 143−148.
(5) Shen, Y. R.; Holzapfel, W. B. Nephelauxetic Effects on Sm^{2+} and Eu^{3+} in Ternary MYX Compounds. *Phys. Rev. B* **1995**, *52*, 12618−12626.
(6) Newman, D. J. Slater Parameter Shifts in Substituted Lanthanide Ions. *J. Phys. Chem. Solids* **1973**, *34*, 541−545.
(7) Albin, M.; Horrocks, W.; De, W. Europium(III) Luminescence Excitation Spectroscopy. Quantitative Correlation between the Total Charge on the Ligands and the $^7F_0$ - $^5D_0$ Transition Frequency in Europium(III) Chelates. *Inorg. Chem.* **1985**, *24*, 895−900.
(8) Amberger, H.-D.; Reddmann, H.; Hagen, C. Electronic Structures of Highly Symmetrical Compounds of f-Elements. XXXIX. Do More Covalent Europium(III) Compounds Exhibit an Anti-Nephelauxetic Behavior? *Inorg. Chim. Acta* **2005**, *358*, 3745−3752.
(9) Frey, S. T.; Horrocks, W. DeW. On correlating the Frequency of the $^7F_0$ - $^5D_0$ Transition in Eu^{3+} Complexes with the Sum of the "Nephelauxetic" Parameters for all of the Coordinating Atoms. *Inorg. Chim. Acta* **1995**, *229*, 383−390.
(10) Bünzli, J.-C.; Chauvin, A.-S.; Kim, H. K.; Deiters, E.; Eliseeva, S. V. Lanthanide Luminescence Efficiency in Eight- and Nine-Coordinate Complexes: Role of the Radiative Lifetime. *Coord. Chem. Rev.* **2010**, *254*, 2623−2633.
(11) Puntus, L. N.; Lyssenko, K. A.; Antipin, M. Y.; Bünzli, J.-C. Role of Inner- and Outer-Sphere Bonding in the Sensitization of Eu-Luminescence Deciphered by Combined Analysis of Experimental Electron Density Distribution Function and Photophysical Data. *Inorg. Chem.* **2008**, *47*, 11095−11107.
(12) Piguet, C.; Bünzli, J.-C.; Bernardinelli, G.; Hopfgartner, G.; Petoud, S.; Schaad, O. Lanthanide Podates with Predetermined Structural and Photophysical Properties: Strongly Luminescent Self-Assembled Heterodinuclear d-f Complexes with a Segmental Ligand Containing Heterocyclic Imines and Carboxamide Binding Units. *J. Am. Chem. Soc.* **1996**, *118*, 6681−6697.
(13) Petoud, S.; Bünzli, J.-C.; Schenk, K. J.; Piguet, C. Luminescent Properties of Lanthanide Nitrato Complexes with Substituted Bis(benzimidazolyl)pyridines. *Inorg. Chem.* **1997**, *36*, 1345−1353.
(14) Choppin, G. R.; Wang, Z. M. Correlation between Ligand Coordination Number and the Shift of the $^5D_0$ - $^7F_0$ Transition Frequency in Europium Complexes. *Inorg. Chem.* **1997**, *36*, 249−252.
(15) Malta, O. L.; Batista, H. J.; Carlos, L. D. Overlap Polarizability of a Chemical Bond: a Scale of Covalency and Application to Lanthanide Compounds. *Chem. Phys.* **2002**, *282*, 21−30.
(16) Souza, A. P.; Rodrigues, L. C. V.; Brito, H. F.; Alves, S., Jr.; Malta, O. L. Novel Europium and Gadolinium Complexes with Methaneseleninate as Ligand: Synthesis, Characterization and Spectroscopic Study. *Inorg. Chem. Commun.* **2012**, *15*, 97−101.
(17) Hölsä, J.; Leskelä, T.; Leskelä, M. Luminescence Properties of Europium(3+)-Doped Rare-Earth Oxyhydroxides. *Inorg. Chem.* **1985**, *24*, 1539−1542.
(18) Takushi, E.; Kushida, T. Anomalous Spectral Properties of Inhomogeneously Broadened Transitions of Eu^{3+} in $Ca(PO_3)_2$ Glass. *J. Lumin.* **1979**, *18/19*, 661−664.
(19) Kushida, T. Transition Mechanisms and Spectral Shapes of the $^5D_0$ - $^7F_0$ Line of Eu^{3+} and Sm^{2+} in solids. *Phys. Rev. B* **2002**, *65*, 195118 (1−6).
(20) Kushida, T. Site-Selective Fluorescence Spectroscopy of Eu^{3+} and Sm^{2+} Ions in Glasses. *J. Lumin.* **2002**, *100*, 73−88.
(21) Tanaka, M.; Nishimura, G.; Kushida, T. Contribution of J Mixing to the $^5D_0$ - $^7F_0$ Transition of Eu^{3+} Ions in Several Host Matrices. *Phys. Rev. B* **1994**, *49*, 16917−16925.
(22) Nishimura, G.; Tanaka, M.; Kurita, A.; Kushida, T. $^5D_0$ - $^7F_0$ Transition Mechanism of Eu^{3+} in $Ca(PO_3)_2$ Glass, Y_2O_2S Crystal and Polyvinyl Alcohol. *J. Lumin.* **1991**, *48&49*, 473−476.
(23) Dexpert-Ghys, J.; Piriou, B.; Jacquet-Francillon, N.; Sombret, C. Europium Site Selective Spectroscopy of Aluminoborosilicate Glasses: Structural Approach and Influence of Phosphorus on the Environment of the Lanthanide. *J. Non-Cryst. Solids* **1990**, *125*, 117−128.
(24) Balda, R.; Fernández, J.; Eilers, H.; Yen, W. M. Site-selective Spectroscopy of Eu^{3+} Ions in Fluoride Glasses. Site-Selective spectroscopy of Eu^{3+} in Fluoride Glasses. *J. Lumin.* **1994**, *59*, 81−87.
(25) Malta, O. L.; Antic-Fidancev, E.; Lemaitre-Blaise, M.; Milicic-Tang, A.; Taibi, M. The Crystal Field Strength Parameter and the Maximum Splitting of the $^7F_1$ Manifold of the Eu^{3+} Ion in Oxides. *J. Alloys Compd.* **1995**, *228*, 41−44.
(26) Zhang, W.-W.; Yin, M.; He, X.-D.; Gao, Y. -Q. Size Dependent Luminescence of Nanocrystalline Y_2O_3:Eu and Connection to Temperature Stimulus. *J. Alloys Compd.* **2011**, *509*, 3613−3616.
(27) Ma, C.-G.; Brik, M. G.; Kiisk, V.; Kangur, T.; Sildos, I. Spectroscopic and Crystal-Field Analysis of Energy Levels of Eu^{3+} in SnO_2 and Comparison with ZrO_2 and TiO_2. *J. Alloys Compd.* **2011**, *509*, 3441−3451.
(28) Görller-Walrand, C.; Binnemans, K. In *Handbook on the Physics and Chemistry of Rare Earths*; Gschneidner, K. A., Jr., Eyring, L., Eds.; Elsevier Science B. V.: 1996; Vol. *23*, p 164.
(29) Moune, O. K.; Cao, P. Computer Simulation of the ^5D_J levels of $4f^6$, Eu^3. *J. Less-Common Met.* **1989**, *148*, 181−186.
(30) Caro, P.; Beaury, O.; Antic, E. L'Effet Néphélauxétique pour les Configurations $4f^N$ en Phase Solide. *J. Phys. (Paris)* **1976**, *37*, 671−676.
(31) Dexpert-Ghys, J.; Faucher, M.; Caro, P. Site-Selective Excitation, Crystal-Field Analysis, and Energy transfer in Europium-Doped Monoclinic Gadolinium Sesquioxide. A Test of the Electrostatic Model. *Phys. Rev. B* **1981**, *23*, 607−617.
(32) Judd, B. R. Three-Particle Operators for Equivalent Electrons. *Phys. Rev.* **1966**, *141*, 4−14.

(33) Duan, C.-K.; Tanner, P. A. What Use are Crystal Field Parameters? A Chemist's Viewpoint. *J. Phys. Chem. A* **2010**, *114*, 6055−6062.
(34) Wen, H.; Duan, C.-K.; Jia, G.; Tanner, P. A.; Brik, M. Glass Composition and Excitation Wavelength Dependence of the Luminescence of Eu^{3+} Doped Lead Borate Glass. *J. Appl. Phys.* **2011**, *110*, 033536 (1−8).
(35) Shen, Y.; Li, C.; Costa, V. C.; Bray, K. L. Laser Site-Selective Excitation Spectroscopy of Eu^{3+}-Doped Yttrium Aluminium Garnet. *Phys. Rev. B* **2003**, *68*, 01401.
(36) de Sagey, G. T.; Porcher, P.; Garon, G.; Caro, P. In *The Rare Earths in Modern Science and Technology*; McCarthy, G. J., Silber, H. B., Rhyne, J. J., Eds.; Plenum: 1982; Vol. 3, pp 127−130.
(37) Yeung, Y. Y.; Tanner, P. A. New Analyses of Energy Level Datasets for $LaCl_3$:Ln^{3+} (Ln = Pr, Nd, Er). submitted.
(38) Morosin, B. Crystal Structures of Anhydrous Rare-Earth Chlorides. *J. Chem. Phys.* **1968**, *49*, 3007−3012.
(39) Binnemans, K.; Görller-Walrand, C. Polarized Absorption Spectra of $Eu(BrO_3)_3.9H_2O$. *J. Phys.: Condens. Matter* **1996**, *8*, 1267−1279.
(40) Thorne, J. R. G.; Jones, M.; McCaw, C. S.; Murdoch, K. M.; Khaidukov, N. M. Two-Photon Spectroscopy of Europium(III) Elpasolites. *J. Phys:. Condens. Matter* **1999**, *11*, 7851−7866.
(41) Tanner, P. A.; Liu, Y.; Edelstein, N. M.; Murdoch, K.; Khaidukov, N. M. Vibrational and Electronic Spectra of EuF_6^{3-}. *J. Phys.: Condens. Matter* **1997**, *9*, 7817−7836.
(42) Görller-Walrand, C.; Binnemans, K.; Fluyt, L. Crystal-Field Analysis of Eu^{3+} in $LiYF_4$. *J. Phys.: Condens. Matter* **1993**, *5*, 8359−8374.
(43) Karbowiak, M.; Zych, E. Hölsä, Crystal-Field Analysis of Eu^{3+} in Lu_2O_3. *J. Phys.: Condens. Matter* **2003**, *15*, 2169−2181.
(44) Xiao, Q.; Liu, Y.; Liu, L.; Li, R.; Luo, W.; Chen, X. Eu^{3+}-Doped In_2O_3 Nanophosphors: Electronic Structure and Optical Characterization. *J. Phys. Chem. C* **2010**, *114*, 9314−9321.
(45) Binnemans, K.; Görller-Walrand, C. Optical Absorption Spectra of Eu^{3+} in $Y_3Ga_5O_{12}$ (YGG). *J. Phys.: Condens. Matter* **1997**, *9*, 1637−1648.
(46) Binnemans, K.; Görller-Walrand, C. Magnetic Circular Dichroism and Optical Absorption Spectra of Eu^{3+} in $Y_3Al_5O_{12}$ (YAG). *J. Chem. Soc., Faraday Trans. 2* **1996**, *92*, 2487−2493.
(47) Hopkins, T. A.; Bolender, J. P.; Metcalf, D. H.; Richardson, F. S. Polarized Optical Spectra, Transition Line Strengths, and the Electronic Energy-Level Structure of $Eu(dpa)_3^{3-}$ Complexes in Single Crystals of Hexagonal $Na_3[Yb_{0.95}Eu_{0.05}(dpa)_3]\cdot NaClO_4\cdot 10H_2O$. *Inorg. Chem.* **1996**, *35*, 5347−5355.
(48) Kirby, A. F.; Richardson, F. S. Detailed Analysis of the Optical Absorption and Emission Spectra of Eu^{3+} in the Trigonal (C_3) $Eu(DBM)_3.H_2O$ system. *J. Phys. Chem.* **1983**, *87*, 2544−2556.
(49) Görller-Walrand, C.; Hendrickx, I.; Fluyt, L.; Gos, M. P.; D'Olieslager, J.; Blasse, G. Optical Spectra and Crystal-Field Analysis of Europium Double Nitrates. *J. Chem. Phys.* **1992**, *96*, 5650.
(50) Görller-Walrand, C.; Huygen, E.; Binnemans, K.; Fluyt, L. Optical Absorption Spectra, Crystal-Field Energy Levels and Intensities of Eu^{3+} in $GdAl_3(BO_3)_4$. *J. Phys.: Condens. Matter* **1994**, *6*, 7797−7812.
(51) Hammond, R. M.; Reid, M. F.; Richardson, F. S. Comparison of Crystal Field Parameters for $Ln(C_2H_5SO_4)_3.9H_2O$ and $Na_3(Ln(C_4H_4O_5)_3).2NaClO_4.6H_2O$ Systems. *J. Less-Common Met.* **1989**, *148*, 311−319.
(52) Berry, M. T.; Schwieters, C.; Richardson, F. S. Optical Absorption Spectra, Crystal-Field Analysis, and Electric Dipole Intensity Parameters for Europium in $Na_3[Eu(ODA)_3].2NaClO_4.6H_2O$. *Chem. Phys.* **1988**, *122*, 105−124.
(53) Karbowiak, M.; Mondry, A. Electronic Energy-Level Structure of $4f^6$ Configuration in Europium(III) Triacetate Tetrahydrate. *Chem. Phys.* **2008**, *354*, 86−93.
(54) Binnemans, K.; Görller-Walrand, C. Crystal Field Analysis of $EuCl_3.6H_2O$. *J. Alloys Compd.* **1997**, *250*, 326−331.
(55) Jayasankar, C. K.; Richardson, F. S.; Reid, M. F. Phenomenological Spin-Correlated Crystal-Field Analyses of Energy Levels in Ln^{3+}:$LaCl_3$ Systems. *J. Less-Common Met.* **1989**, *148*, 289−296.
(56) Chen, X. Y.; Liu, G. K.; Margerie, J.; Reid, M. F. A Few Mistakes in Widely Used Data Files for f^n Configurations Calculations. *J. Lumin.* **2008**, *128*, 421−427.
(57) Dushin, R. B.; Barbanel, Yu A.; Kolin, V. V.; Kotlin, V. P.; Nekhoroshkov, S. N.; Chudnovskaya, G. P. Luminescence Spectra of $Cs_2NaLuBr_6$:Eu^{3+} Crystal. *Radiochemistry* **2000**, *42*, 53−60.
(58) Li, W.; Ning, L.; Tanner, P. A. Double Perovskite Structure: a Vibrational and Luminescence Investigation Providing a Perspective on Crystal Field Strength. *J. Phys. Chem. A* **2012**, *116*, 7337−7344.